

Annular symmetry nonlinear frequency converters

Dror Kasimov, Ady Arie, Emil Winebrand, Gil Rosenman

School of Electrical Engineering, Faculty of Engineering, Tel-Aviv University, Ramat Aviv, Tel-Aviv, Israel 69978

Ariel Bruner, Pnina Shaier and David Eger

Electro-Optics Division, Soreq NRC, Yavne 81800, Israel

Abstract: We present a new type of two-dimensional nonlinear structure for quasi-phase matching. This structure has continuous rotational symmetry, and in contrary to the commonly used periodic structures, is not lattice shaped and has no translation symmetry. It is shown that this annular symmetry structure possesses interesting phase matching attributes that are significantly different than those of periodic structures. In particular, it enables simultaneous phase-matched frequency doubling of the same pump into several different directions. Moreover, it has extremely wide phase-mismatch tolerance, since a change in the phase matching conditions does not change the second harmonic power, but only changes its propagation direction. Several structures were fabricated using either the indirect e-beam method in LiNbO_3 or the electric field poling method in stoichiometric LiTaO_3 , and their conversion efficiencies, as well as angular and thermal dependencies, were characterized by second harmonic generation.

©2006 Optical Society of America

OCIS codes: (190.2620) Frequency conversion; (190.4360) Nonlinear optics, devices; (160.4330) Nonlinear optical materials.

References and Links

1. M. M. Fejer, G. A. Magel, D. H. Jundt and R. L. Byer, "Quasi phase matched second harmonic generation: Tuning and tolerances," *IEEE J. Quantum Electron.* **28**, 2631-2654 (1992).
2. V. Berger, "Nonlinear photonic crystals," *Phys. Rev. Lett.* **81**, 4136-4139 (1998).
3. N.G.R. Broderick, G.W. Ross, H.L. Offerhaus, D.J. Richardson and D.C. Hanna, "Hexagonally poled lithium niobate: a two-dimensional nonlinear photonic crystal," *Phys. Rev. Lett.* **84**, 4345-4348 (2000).
4. S. M. Saltiel, A. A. Sukhorukov and Y. S. Kivshar, "Multistep parametric processes in nonlinear optics," *Prog. Optics* **47**, 1-73 (2005).
5. Isaac Amidror, "Fourier spectrum of radially periodic images," *J. Opt. Soc. Am. A* **14**, 816-826 (1997).
6. Y. Glickman, E. Winebrand, A. Arie, and G. Rosenman, "Electron-beam-induced domain poling in LiNbO_3 for two-dimensional nonlinear frequency conversion," *Appl. Phys. Lett.* **88**, 011103 (2006).
7. M. Yamada, N. Nada, M. Saitoh, and K. Watanabe, "First-order quasi-phase-matched LiNbO_3 waveguide periodically poled by applying an external field for efficient blue second harmonic generation," *Appl. Phys. Lett.* **62**, 435-436 (1993).
8. Y. Furukawa, K. Kitamura, E. Suzuki and K. Niwa, "Stoichiometric LiTaO_3 single crystal growth by double-crucible Czochralski method using automatic powder supply system," *J. Cryst. Growth* **197**, 889-895 (1999).
9. A. Bruner, D. Eger and S. Ruschin, "Second harmonic generation of green light in periodically-poled stoichiometric LiTaO_3 doped with MgO ," *J. Appl. Phys.* **96**, 7445-7449 (2004).
10. R.W. Boyd, *Nonlinear Optics, second edition*, (Academic press, 2002), Chap. 2.
11. F.W. Byron and R.W. Fuller, *Mathematics of classical and quantum physics*, (Dover publications, 1992), Chap. 7.
12. D. H. Jundt, "Temperature-dependent Sellmeier equations for the index of refraction n_e , in congruent lithium niobate," *Opt. Lett.* **22**, 1553-1555 (1997).

Periodic modulation of the second order nonlinear susceptibility, either in one dimension¹ (1D), or in two dimensions^{2,3,4} (2D) is widely used nowadays for quasi-phase matched (QPM)

frequency conversion. These structures are lattice shaped, and have discrete rotational symmetry, i.e., efficient frequency conversion is achieved only for specific input and output angles. On the other hand, they usually have continuous translation symmetry: translating the frequency converters in a direction perpendicular to the input pump wave usually does not change the power of the generated waves. We present here a new type of nonlinear structure, one that possesses only continuous rotational symmetry and no translation symmetry.

The structure of interest is a binary annular grating. It is a structure of concentric rings alternating between $+d$ and $-d$, where d is a tensor element of the second order nonlinear susceptibility. The normalized, space-dependent part of the nonlinear coefficient can be written analytically as a sign function of a radial cosine.

$$g(r) = \text{sign}(\cos(2\pi r/\Lambda)) \quad (1)$$

where $r = \sqrt{x^2 + y^2}$. To understand its phase matching possibilities, we need to know its Fourier transform¹. The Fourier transform of an infinite structure with a period of Λ consists of concentric impulse rings⁵ with a period of $2\pi/\Lambda$. Figure 1 shows the structure in real space and its Fourier transform. Figure 1(b) also shows an example of the phase matching diagram for second harmonic generation (SHG), in the case where the pump passes exactly at the center of the structure. One can see that phase matching occurs symmetrically from both sides of the pump and that simultaneous phase matching at different orders and angles can occur. The different walk-off angles (angles between the fundamental and the second harmonic) at which we get phase matching are obtained by the law of cosines:

$$\cos \theta_n = \frac{(2k^\omega)^2 + (k^{2\omega})^2 - G_n^2}{4k^\omega k^{2\omega}} \quad (2)$$

where $G_n = n \cdot 2\pi/\Lambda$, and $k^\omega, k^{2\omega}$ the wave-vectors of the fundamental and second harmonic, respectively.

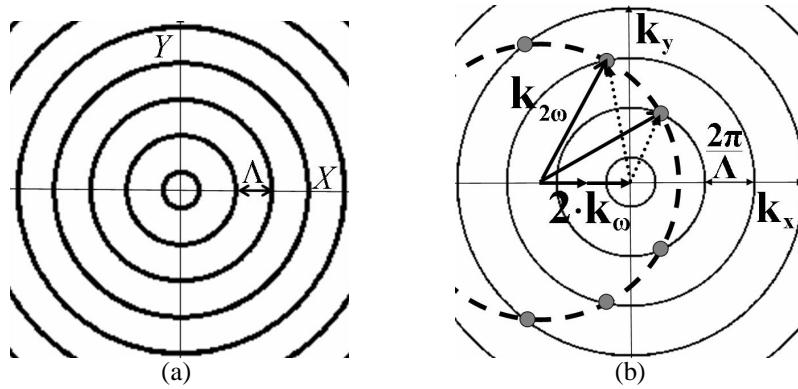


Fig. 1. (a) – The binary annular grating with period Λ . (b) – Fourier transform of the binary annular grating and phase matching diagram for SHG. The second harmonic's k-vector outlines a circle around the fundamental's k-vectors giving all possible phase mismatches. Points of intersection between this circle and the structures Fourier space rings are the points of phase matching (represented by large grey dots).

A change of the phase matching condition (e.g., by changing the temperature or the wavelength) will result in a change of the angles of second harmonic without losing phase matching. This is in contrast to 1D or 2D periodic structures where a change of the phase matching condition will usually result in a sharp efficiency drop as a result of the loss of phase matching. This means that the annular binary structure has a much higher phase mismatch tolerance than periodic QPM structures.

It should be noted that the phase matching considerations shown in Fig. 1 are true when the input beam passes through the center of the structure and for an infinite structure. Other conditions change the structure in the Fourier space, although the general considerations remain true.

Annular symmetry structures can be manufactured using similar methods to those that are used for making periodic nonlinear structures. We fabricated several binary annular structures with various periods using two poling methods – indirect e-beam poling⁶ in LiNbO₃ and electric field poling⁷ in stoichiometric LiTaO₃ (SLT). Two structures were used in second harmonic generation experiments:

(1) An annular binary structure poled on lithium niobate using the indirect e-beam method with a period of 28 μm , having a size of 800x800 microns.

(2) An annular binary structure poled on SLT using the electric field poling with a period of 7.5 μm and an active size of 8.75x5 mm. The period of 7.5 μm was chosen since it enables co-linear QPM SHG of a Nd:YLF laser at 1047.5 μm .

The first structure was accomplished using the indirect e-beam poling method as follows. A 0.5 mm thick z-cut LiNbO₃ crystal of congruent composition was used. A Shipley-1818 photo-resist of 2 μm thickness was spin coated over the crystal C⁻ face. The electron exposure was performed by using a commercial electron beam lithography system (ELPHY Plus) adapted to a JEOL JSM 6400 scanning electron microscope. The acceleration voltage was selected to be 15kV corresponding with the photo-resist dielectric layer thickness so that the majority of incident electrons would stay trapped in the coating layer, therefore inducing high electric field that causes the inversion. The adaption of the electron energy and photoresist thickness was performed using Monte-Carlo simulations to calculate the effective penetration depth of electrons into the layer. The beam current was set to 0.5nA and the deposited surface charge density 300 $\mu\text{C}/\text{cm}^2$. After exposure the resist layer was removed and the crystal was etched for 120 min using hydrofluoric (HF) acid at room temperature to reveal the formed domain structures. The duty cycle of this structure was kept at a relatively low value, around 10%, in order to reduce Coulomb deflection of the electron-beam, caused by the charging of the photo-resist⁶.

The second structure was realized in a 0.5 mm thick z-cut SLT crystal, grown by double-crucible Czochralski⁸, using our standard electric field poling technique as described previously for 1D structures⁹. First, the annular structured pattern of photoresist was contact printed on the C+ face of the wafer from a lithographic mask. Then, the surface was coated by a uniform metallic layer.

The electrical poling was achieved by applying pulses 0.6 kV to the polar crystal surfaces. The total switching charge was 65 $\mu\text{C}/\text{cm}^2$. After poling, the photoresist and the metallic coatings were removed and the domain structure was revealed by HF etching. Most of the structure of the SLT crystal had a duty factor of 70% at the C+ surface and close to 80% at the C⁻ surface, while the period length of 7.5 μm was precisely kept along the crystal. The end faces of the two crystals were polished for the optical measurements. Fig. 2 shows optical and AFM pictures of the surface morphology for the two different crystals.

To validate the stability and accuracy of the period we performed far field diffraction on the field poled structure using a doubled Nd:YAG laser ($\lambda = 532\text{nm}$). The resulting diffraction pattern can be seen in Fig. 3. This pattern was highly periodic which indicates a stable period. The angle to the first circle of diffraction was $\theta \approx 0.0705 \text{ rad}$. By using the well known law of diffraction ($\lambda = \Lambda \sin \theta$) we calculated the period of the structure to be $\Lambda = 7.55 \mu\text{m}$, which agrees well with the design period of 7.5 μm .

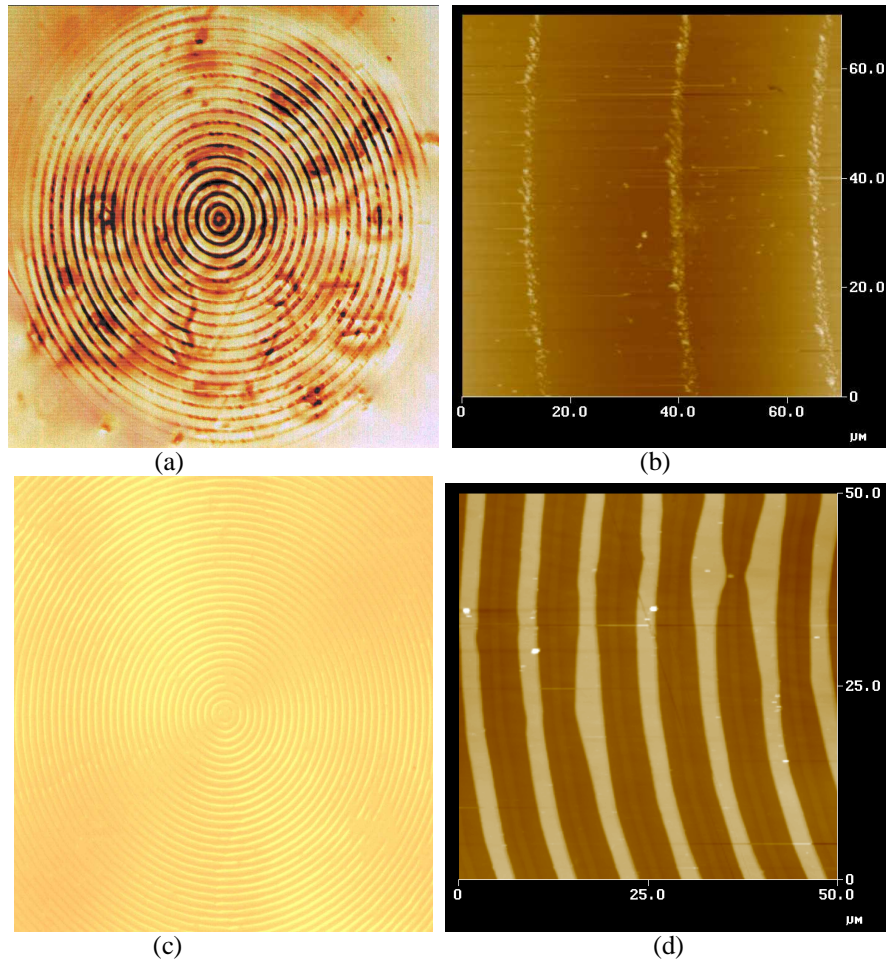


Fig. 2. Optical and AFM pictures of the e-beam poled lithium niobate - (a) and (b) respectively and of the electric field poled SLT - (c) and (d) respectively.

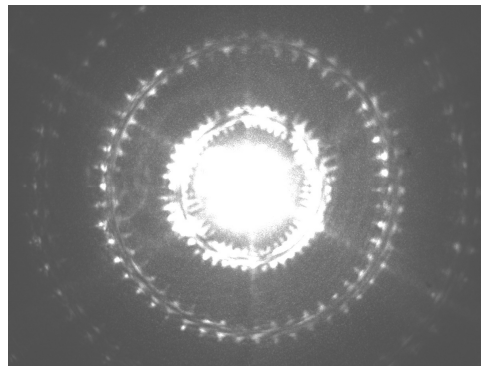


Fig. 3. Diffraction pattern of the electric field poled structure.

The 28 μm structure was used in two SHG experiments with two different pump sources - a 1.0475 μm Q-switched Nd:YLF laser and a PPLN OPO with a pump signal at 1.42 μm . The structure with 7.5 μm period was used only in SHG of the Nd:YLF laser. We measured the angles of second harmonic and the temperature dependence.

Table 1 presents the measured second harmonic angle in the various experiments. For the Nd:YLF laser, only high orders (5 & up) are observed with the (relatively large) 28 μm period structure. But when moving to longer wavelength or a shorter period, phase-matched SHG with lower orders is observed. The theoretical angles were calculated using Eq. (2).

Table 1. Angular measurements in SHG experiments with annular structures

Process	Order	Theoretical angle (degrees)	Measured angle (degrees)
SHG of Nd:YLF. E-beam poled LiNbO ₃ . $\Lambda=28 \mu\text{m}$.	5	2.46	2.5
	6	4.33	4
	7	5.9	6.1
SHG of an OPO signal. E-beam poled LiNbO ₃ . $\Lambda=28 \mu\text{m}$.	2	1.3	1.065
SHG of Nd:YLF. Electric field poled SLT. $\Lambda=7.5 \mu\text{m}$.	1	0	0
	2	7	6.9
	3	11.5	11.5
	4	15.9	16

Table 2 shows the various efficiencies in the experiments performed. These efficiencies are compared to the theoretical efficiencies calculated using the Green's function method, as outlined below. For the structure with 7.5 μm period we assumed that the effective interaction length is 8.75 mm and the duty cycle is 80%, as derived from the microscope and AFM characterization of this sample.

Table 2. Normalized frequency doubling efficiencies

Process	Normalized theoretical efficiency (%/W)	Normalized measured efficiency (%/W)
5 th order. 28 μm period.	1.0e-6	7.7e-8
2 nd order. 28 μm period.	5.2e-6	7.8e-7
1 st order. 7.5 μm period.	3.6e-1	1.5e-1
2 nd order. 7.5 μm period	5.5e-7	1.7e-7

Theoretical efficiencies were calculated using a numerical simulation that solves the Helmholtz equation for a second harmonic process¹⁰. We used the Green's function approach, which in our case is a simple spherical wave¹¹: $G(R) = e^{ikR}/(4\pi R)$, $R = |r - r'|$. The second harmonic wave is obtained by convolution of the Green's function with the source distribution – the non linear polarization

$$\bar{E}^{2\omega}(r) = -\iiint G(R) \frac{(2\omega)^2}{c^2} 2d(\bar{E}^\omega)^2 \cdot dr' \quad (3)$$

where E^ω is the input field (Gaussian beam with 80 μm beam waist), ω is the angular frequency of the input, c is the velocity of light, and d is, as defined earlier, a tensor element of the nonlinear susceptibility.

This method does not require any upfront assumptions on the direction of propagation of the second harmonic wave and is relatively straight-forward and simple. Calculations done using the numerical simulation have shown that in co-linear propagation, the efficiency is very

similar to that of a regular 1D periodic structure. Non-co-linear propagation on the other hand has very low efficiency when compared to periodic structures.

The effect of phase mismatch was studied by altering the device temperature. Fig. 4 shows temperature dependence measured with $7.5\ \mu\text{m}$ structure. Whereas the collinear case shows a clear sinc-like behavior, the non collinear 2^{nd} order behaves very differently and is much less temperature dependent.

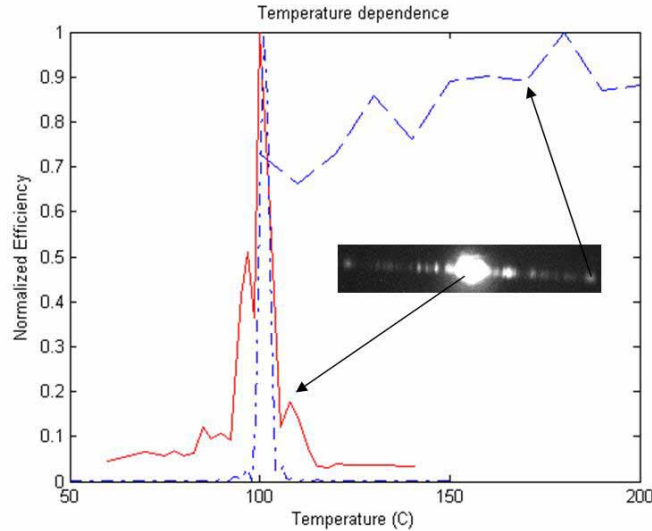


Fig. 4. Temperature dependence of the SHG efficiency in SLT. Solid and dashed lines: measurements of the 1^{st} order (collinear) and 2^{nd} order (non-collinear) interactions, respectively. Dash-dot line: Calculation of the co-linear 1^{st} order. Inset: photo of the SHG signal on a screen. The central spot is the collinear SHG, whereas the side spots represent the non-collinear SHG

We have presented in this article a new type of nonlinear structure for QPM interactions. This structure has continuous rotation symmetry and no translation symmetry, unlike the commonly used periodic nonlinear structures that have continuous translation symmetry and discrete rotation symmetry. Because of its symmetry properties, the angle of entrance (disregarding refraction) does not change its phase matching properties. On the other hand, the point of entry to the structure is highly important, and the device will work most efficiently when passing exactly through the center of the rings. This is exactly opposite in normal lattice-like structures where the angle matters but point of entry does not. Also in annular structures several orders and/or processes can be present simultaneously at different angles. This does not usually happen in lattice-like structures where a change of angle or temperature is needed in order to phase-match at another order. Probably the most significant difference between this new structure and previous structures is its behavior with a change of the phase mismatch. Such a change will result in a change of the angles of second harmonic, without losing phase matching and not in a sharp loss of efficiency as in periodic structures.

The low dependence of the annular structure on phase mismatch can be useful for easing the restrictions on exact period length for specific processes when working non co-linearly. A slight change in the period will only result in a slight change of the walk-off angle and not in a sharp efficiency change. These structures can therefore be used to measure dispersion relations for non-linear crystals. By measuring different angles and orders at various wavelengths and temperatures we can deduce the refraction coefficients of the crystal at a wide span of conditions¹².

Acknowledgments

This work was partly supported by the Israel Science Foundation, grant no. 960/05.